Computational Structural Optimization and Digital Fabrication of Timber Beams

Paul L. MAYENCOURT*, Joaquin S. GIRALDO[a], Eric WONG[a], Caitlin T. MUELLER[a]

*Massachusetts Institute of Technology
77 Massachusetts Avenue, Cambridge, MA, USA
mapaul@mit.edu

[a] Massachusetts Institute of Technology

Abstract

This paper focuses on optimizing beams made of solid timber sections through a CNC subtractive milling process. An optimization algorithm shapes beams and reduces the material quantities by up to 50% of their initial weight. A series of these beams are then fabricated and load tested, and their strength is compared to standard timber sections.

Keywords: Timber Structures, Digital Fabrication, Shape Optimization, Computation Structural Optimization, CNC, Load testing.

1. Introduction

In a world of limited resources, engineers and architects cannot fail to optimize material usage and energy in structures. The building sector contributes to approximately 40% of the global greenhouse gas emissions (EIA [1]). The energy consumption in building is divided between operational and embodied energy. The operational energy is the energy consumption over the entire lifespan of a building that goes into cooling, heating, lighting, etc. The embodied energy is the necessary energy to construct the building, such as the manufacturing of structural materials, transportation of building components, etc. There are two pathways for designers to reduce the embodied carbon in buildings: material minimization and low embodied carbon materials. The low embodied carbon structural material pathway aims to use more environmentally efficient structures such as timber or masonry (De Wolf [2]). Structural optimization achieves material savings with more efficient use of material through geometrical and topological changes (Spillers and McBain [3]). While this often results in shapes difficult to build, digital tools are increasingly offering possibilities to build complex structures at marginal added costs.

A key opportunity for material savings in buildings lies in structural components in bending, especially in beams. Bending is the least efficient structural action, compared to pure tension and compression. However, bending is ubiquitous in the built environment as it allows for spans with flat floors and roofs, and easily resolved support conditions. In this context, beam shaping appears to be an efficient structural design method to save materials (Allen and Zalewski [4], Engel [5]). Connected to modern fabrication methods as such as additive or subtractive manufacturing, shaped beams could significantly reduce the amount of material used in buildings. Finally, reducing the weight of bending systems has the potential to reduce dead loads and hence the size of the columns and foundations for multistory or high-rise buildings.

This paper explores old and new techniques for shaping beams. The scope is limited to simply supported timber beams, using subtractive manufacturing. The first part reviews current research and structural optimization methods for beam shaping. The second part describes the analytical and computational design used in this paper. The last part presents fabrication and load testing results on prototypes.

2. Literature review

In 1638, Galileo Galilei discovered the action of bending stresses in cantilever. With this, he explored the possibility of shaping beams according to the stress distribution. For a cantilever with a single point load at the tip, the beam takes the shape of a square root function (Timoshenko [6]).
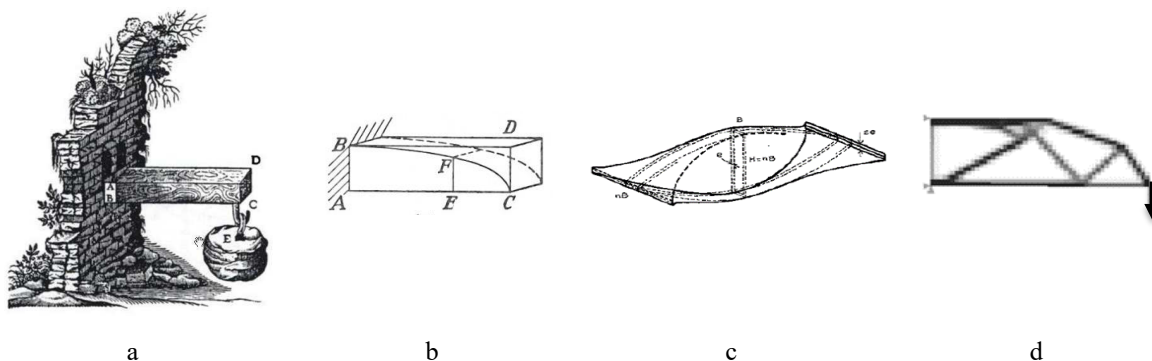

| a | b | c | d |

Figure 1: a, b: Galileo's study on the shape of a cantilever beam in his 1638 publication, Timoshenko [6], c: simply supported beam optimized for weight, P. Samyn [7], d: topology optimization of a cantilever with point load at tip [8].

More contemporary research has investigated the analytical solutions for simple beams (Samyn [7]). In this case, the analytical equations for different loading cases and beam geometries are solved. Although offering a wide range of interesting optimal designs, this results in either theoretical shapes difficult to build or geometries unfit for buildings, as little control can be applied on the shape.

A wide range of numerical tools and methods has been developed for structural optimization. Topological optimization of structures solves the problem of distributing a finite quantity of material within a given boundary to achieve a structural goal (Bendsoe and Sigmund [9]). While current tools offer interactive design tools for designers (Aage et al. [8]), the resulting geometries often require post-processing and rationalization for construction. Moreover, the designer has little control over the final shape of the structure. On the contrary, structural shape optimization optimizes the geometry of a predefined topology. While this has many advantages for constructability, the design space is more restrained. In literature, this method has been used to form find shell structures, for example. In this case, the shell geometry is defined by a series of Non-Uniform Rational Basis Splines (NURBS) or NURBS-surface. The control points of the 3D curves are used to modify the geometry under a set of constraints in order to minimize an objective function with an evolutionary algorithm (Cui et al [10]).

Beam shaping linked to fabrication methods and specific materials has been used in current research as a means towards producing more efficient structural elements. Fabric formwork for optimal concrete structure has gained a lot of popularity in recent years (West [11]), using the same NURBS-based approach. The hydrostatic pressure of the fresh concrete forms the fabric into an optimized beam shape. This requires an adequate control of the boundary conditions and the pattern of the fabric. While the method enables to build efficient structural shape simply with very little formwork, the final shape of the beam is governed by the hydrostatic pressure action and the boundary conditions of the fabric formwork. More generally, custom timber formwork has been used to build shaped concrete beams. However, optimal geometries are difficult to achieve with straight wood boards or panels. CNC-milled formwork or curved panels are certainly possible, but at a higher cost premium.

In conclusion, optimization methods are available to improve the efficiency of structures. While work exists in beam optimization for concrete and steel sections, little has been done to link these techniques with structural timber.

3. Methodology

This section investigates the use of analytical solutions for beam shaping and then proposes a numerical approach. For the scope of this paper, a simply supported beam with a point load at its center is considered. The optimization aims to reduce the structure's volume.

3.1. Analytical and computational design

Two methods are used for the beam section optimization. The first one derives the shape of the beam using analytical solutions, inspired from G. Galilei and refers to the traditional optimization theory (Haftka and Karnat [12]). The second method uses computational structural shape optimization.

3.1.1. Analytical beam shaping for constant stress

The equation of the bending stress $\sigma(x)$ along the beam axis, given a moment distribution for a rectangular-sectioned beam of width *b* and height *h* is as follow:

$$\sigma(x) = \frac{6M(x)}{b(x)h(x)^2} \tag{1}$$

where *M(x)* is the bending moment along the beam axis. The unknowns in the equation are *b(x)* and *h(x)*. With only one equation, one of the parameters has to be fixed in order to solve for the other. The bending stress is set such as $\sigma = \sigma_{max,\ allowable}$.

If the width is set constant *b(x) = b*, it can solved for *h(x)*:

$$h(x) = \sqrt{\frac{6M(x)}{b\sigma}} \tag{2}$$

If the height is set constant *h(x) = h*, it can be solved for *b(x)*:

$$b(x) = \frac{6M(x)}{h^2\sigma} \tag{3}$$

The last option to solve the equation (1) is to fix the aspect ratio of the cross section *h(x) = f(x)b(x)*, where *f(x)* is a non-zero function. Contrarily to above, the designer has more control on the shape of the beam with the choice of the function cross sectional ratio function *f(x)*. For a constant cross-section aspect ratio function, the generated volume does not always fit in the initial bounding box and is therefore not used for the following comparison.

Figure 2 compares the two analytical methods and their relative savings to the initial bounding box. The considered system is a simply supported beam, with a point load at mid-span. In each case, the shear stress contribution was added (influences the height close to the supports). The span is 1 m, the load 2.5 kN, the maximal elastic bending stress 5.34 N/mm^2 and the shear stress 0.9 N/mm^2. The initial cross section is 13.97 cm by 3.87 cm. This corresponds to a 2 by 6-inch (nominal) section of low-grade timber Spruce-Pine-Fir South (SPFs). Since the solution using the cross-section aspect ratio function varies with the input function and doesn't fit in the initial bounding box, it is not used for comparison here.
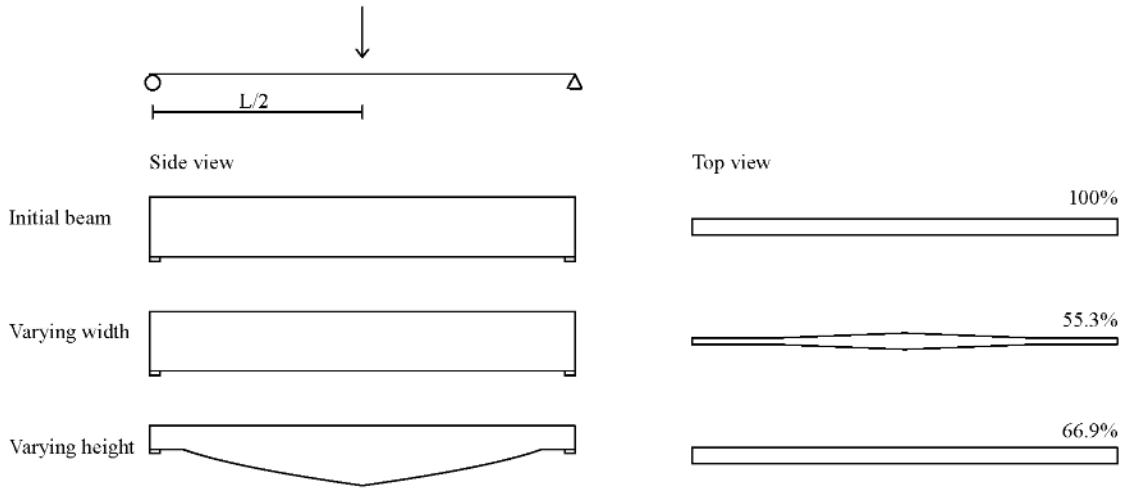
Figure 2: Optimized beams with varying width or height

It is interesting to note that shaping the width of the beam, starting from an initial bounding box, is more efficient in reducing the weight than shaping the height. In fact, the height contributes more to the resistance (h^2). If the full height is conserved, more volume in the width can be removed.

While displacement can be the determining factor in timber structures, the displacement constraint has not been implemented for the scope of this paper.

3.1.2. Numerical optimization method

The numerical method developed in this paper is an extension of the previous examples ([10], [11]). The general strategy used here is a parametric variation of the beam's width and height along its axis. The method is implemented using the 3D modeling software Rhinoceros 5 [13] and Grasshopper for Rhino5 [14].

3.1.2.1. Geometrical model

The beam section is defined with a set of three dimensional curves. The beam's *x* axis is divided into points. Each point is contained by a plan perpendicular to the beam's main axis. In this plan, a set of points is defined parametrically by its (*y*, *z*) coordinates. The initial bounding defines the upper and lower bound of the variables. A curve is interpolated between the corresponding points of the planes, which are then used as control points (3rd degree curve). The entire volume is defined by the number of divisions in the beam's axis and the number of division in the section's height. A volume is lofted between the curves to generate the beam's volume. The use of symmetry at the center of the beam and in the cross section enables the reduction of the number of variables. Cross-sectional properties are extracted with the Rhino built-in command for beam slices along the volume's axis. From the section properties, the bending and shear stress distribution can be computed using the general following formulas:

$$\sigma_{bending} = \frac{M(x)}{W(x)} \ and \ \tau_{shear} = \frac{V(x)}{A_V(x)} \tag{4}$$

With *M(x)* the moment distribution, *W(x)* the section modulus along the beam axis, *V(x)* the shear distribution and $A_v(x)$ the shear area at point *x*. By varying the *y* and *z* coordinates of the control points, the beam volume can be linked to an optimization algorithm.
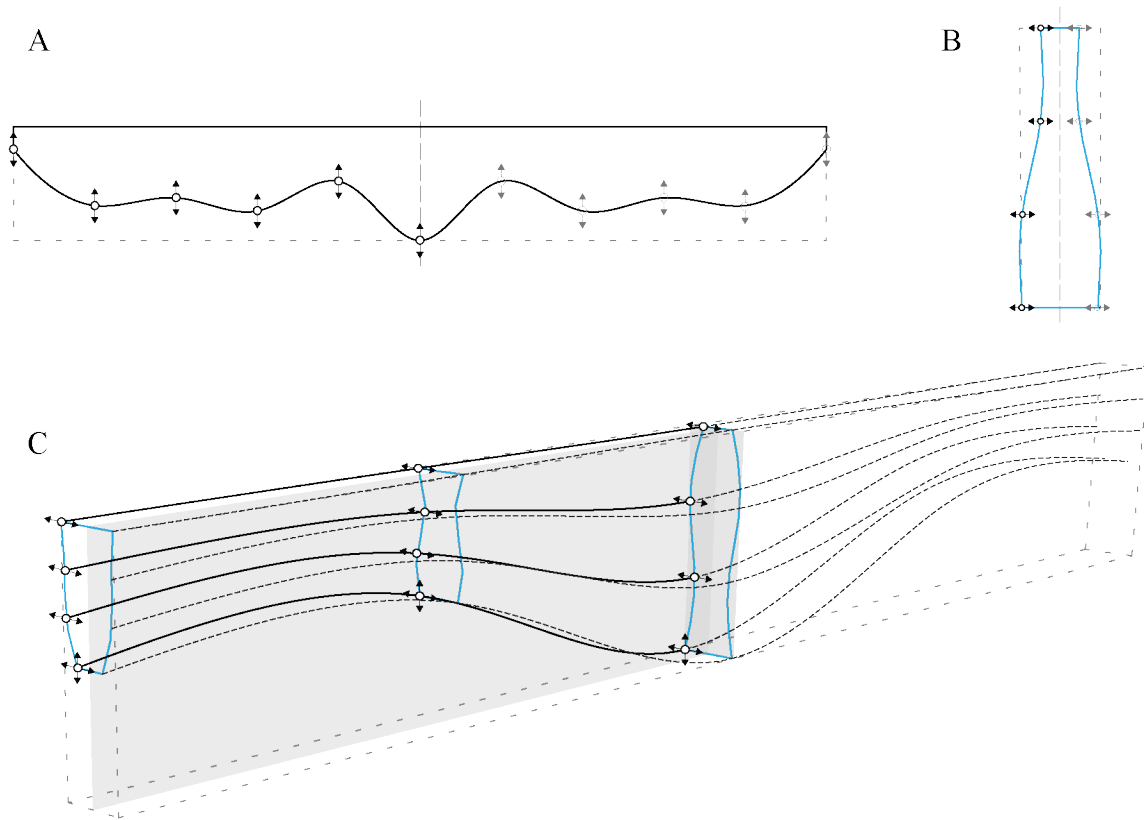
Figure 3: Generation of the beam volume for the optimization. A: shaping height only with symmetry at the center. B: Shaping width only, with mirroring of the cross-section. C: Shaping height and width at the same time. The quarter of the beam is mirrored twice.

The different numerical shaping methods are illustrated in Figure 3. The first method shapes the beam in height only (A), here exemplified with 6 variables. The second method (B) enables the section's width to vary, but the height remains constant (shown here with four variables). Finally, the last method (C) allows to vary the width and the height of the beam along its axis. In this third example, 12 variables for the width and three variables for the height are used. If the beam defined by the bounding box is designed for the maximal load that the shaped beam has to support, the cross section at the center can be fixed to its maximal to reduce the number of variables. Furthermore, the section can be defined with an additional symmetry axis to further reduce the number of constraints and increase the definition of the shape. However, this implies that the beam is not flat at the top.

3.1.2.2. Optimization

An optimization algorithm minimizes the beam's volume under a set of constraints.

$$\min W(x)(1 + \sum P(x)) \tag{5}$$

where $W(x)$ is the material volume, and $\Sigma P(x)$ is sum of the penalty jump functions, illustrated here in the case of the bending stress as:

$$P(x) = \begin{cases} 0 \text{ if } \sigma(x) < \sigma_{allowable} \\ 10^8 \text{ if } \sigma(x) \geq \sigma_{allowable} \end{cases} \tag{6}$$

P(x) can be extended to more general constraints that include displacement limits, for example. The coordinates of the control points along the beam axis define the design space of the optimization problem. The coordinates are bound by an initial volume. The problem is generally defined with 6 to 30 variables. The global evolutionary solver (CSR2) of Goat (Flöry et al [15]) for Grasshopper is used to run the optimization. Once a satisfactory solution is found, the local quadratic approximations solver (BOBYQA) of the same plugin is used to further refine the solution.

3.1.3. Short Discussion and comparison

For a given initial beam volume, the different shaping methods are compared. The chosen material properties are $\sigma_{bending}$=5.34 N/mm^2, P=2.5 kN, the span is 1 m. The final volumes of the beam are compared in the following table:

Table 2: Comparison of the volume savings for the analytical and NURBS-based approaches for a simply supported beam with point load at mid-span.

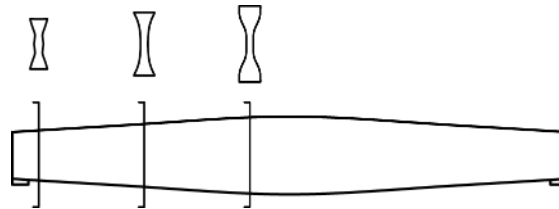| Initial volume	Analytical solution		Numerical Solution		
	Varying height	Varying width	Varying height (5 variables)	Varying width (5 variables)	Varying height and width (13 variables) 3 planes of symmetry
100%	66.9%	55.3%	68.7%	57.5%	49.3%

Figure 4: Optimized beam using the numerical approach where width and height are shaped at the same time. The weight is reduced by more than half of the initial volume.

From the results, we see that the numerical approach is very close to the analytical results when comparing the same cases. However, a more refined version, with more variables, would get closer to the analytical solution.

In this model, the shear stress model is simplified and the material is considered to be a homogenous elastic material. In order to apply this method to timber beams, the idealized beam model needs to take into consideration limitations due to the material properties of timber and the fabrication method.

3.2. Adjusting to timber fiber properties

In order to take into account the weakening due to the fiber discontinuity in the wood on the cut side, the equation based on Hankinson [16] and Kollman [17] is used for the cut side of the beam in tension. The angle between the fiber and the cut direction is extracted from the geometry.
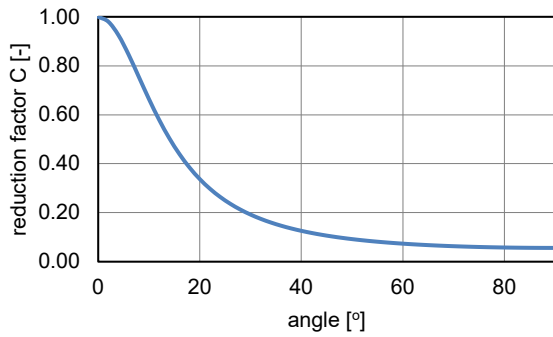
$$f_{t,\alpha} = C_{t,\alpha}\, f_{t,\|} \qquad (7)$$

$$C_{t,\alpha} = \frac{f_{t,\perp}}{f_{t,\|}\sin(\alpha)^2 + f_{t,\perp}\cos(\alpha)^2} \qquad (8)$$

$f_{t,\alpha}$:   resistance outside the main fiber direction, at an angle α.

$C_{t,\alpha}$:   reduction factor.

$f_{t,\|}$:   resistance in tension, parallel to the main fiber direction.

$f_{t,\perp}$:   resistance in tension, perpendicular to the main fiber direction.

Figure 5: Reduction factor for timber loaded diagonally to of the main longitudinal axis (fiber axis).

3.3. General fabrication constraints

Although current digital fabrication tools are very versatile and allow designers to construct a wide range of design more simply, these fabrication methods still have limitations. In this case, a subtractive milling process was used to carve the shaped beam from an initial volume. The fabrication is realized on a small scale ShopBot BT32 Buddy 32''.

The fabrication constraints were built into the beam volume definition. In the case of the table CNC, the points only had a lateral degree of freedom to ensure that the beam could be milled from both sides (flip milling) and reached by the router bit.

4. Results

The results of the numerical shaping method applied to the timber beams are discussed in this section. The numerical optimization was performed on a timber beam with a span of 1m. The design load for the low grade Spruce-Pine-Fire South (US Grade 2) section (3.8 cm by 13.6 cm) is 2.5 kN. The maximal bending strength assumed is 5.34 N/mm^2, the design shear stress is 0.9 N/mm^2 and the resistance in tension perpendicular to the fiber is taken as 0.3 N/mm^2. The initial section was used as a bounding box for the shaping algorithm. The beam was optimized by shaping the height only, using the fiber adjustment properties described above. The resulting beam is 19% less volume than then initial, full-section beam.

4.1 Fabrication: shaping height only

The results from the fabrication process are shown in Figure 6. On the left, the initial beam corresponds to the bounding box used for the optimization. On the right, the shaped beam is 19% lighter than then initial beam. The beam was milled in under a minute.


Figure 6: Left: initial beam. Right: timber beam shaped for height

4.2 Load testing: shaping height only

The shaped and initial beams were load-tested for verification in a three points bending test on a set of three specimens for each case. The results are shown in Figure 7. The results confirm the prediction for the design load of 2.5 kN: both the shaped beam and initial section achieve the design load. The ultimate

load of the beam is much higher than the predicted load, as the design value corresponds to the fifth percentile of the resistance for the selected grade. However, the ultimate load for the shaped and initial beams are different. In fact, the current model is based on elasticity theory, assuming that the section remains planar up to the elasticity limit of the material. The ultimate load goes beyond this limit, as it can be seen from the ductile behavior of the 'full beams' when the curves flatten. Moreover, shaping the beams removes alternative load paths, as the beam is designed to take exactly the design load. This translates into a greater sensitivity to defects (such as knots) and could explain the difference in ultimate loads. Finally, the simplified model for shear stress does not take into account the effect of the beam's slope on the shear stress distribution.
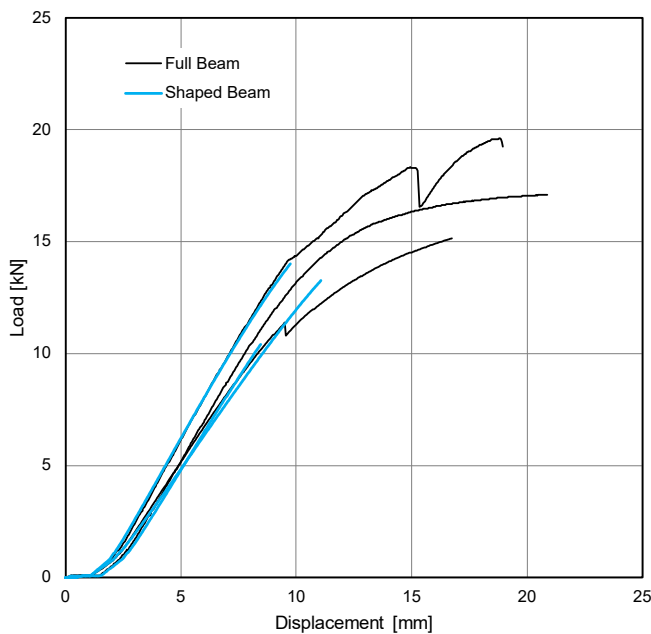
Average displacement at 2.5 [kN]	
Full beams	Shaped beams
3.26 [mm]	3.32 [mm]

Figure 7: Results from the three points bending load test. In the elastic range, the shaped beam with a volume reduction of 19% shows similar behavior to the unshaped version.

To summarize, the predicted design load could be achieved for the shaped beams, with a similar behavior in the elastic region, while saving 19% of the weight.

4.3 Fabrication: shaping height and width

The fabrication of prototypes with varying width and height was carried out in order to experiment with flip milling. In this case, the first face of the beam is milled in on operation. Then, the beam is flipped on the CNC table and positioned carefully to the same location using guides. Finally, the second face is milled with a new milling operation. The prototype is shown in Figure 8. It took 20 minutes to mill each face of the beam.

Figure 8: Prototype of a beam shaped in the height and width

4.4. Discussion

The analytical solution is fast and efficient in shaping beam volumes. However, the design possibilities are limited. The numerical optimization method effectively shapes the beams to reduce their weight as well, while expanding the solution space of shaped beams. The fabrication was successfully implemented to build the prototypes. More interesting and lighter designs are obtained with more design variables. Shaping the height results in very fast milling time. Moreover, shaping the width increases the savings but also increases the milling time, as the two faces have to be machined. The speed of fabrication in relation to the savings achieved should be judged on prototypes at building scale to better balance the benefits of a more complex milling for greater volume saving. Also, industrial CNC machines are far more efficient. In this case, the tool path was not optimized for speed of fabrication.

In general, robotic fabrication has a minimal running cost, but this cost should be compared to cost savings due to lighter bending systems. The current fabrication method removes material from an initial beam volume. As wood comes in square sections to start with, the removal process is beneficial for the total dead loads of the structural system. The wood shavings can be reused for wood products (fibreboards), as a fuel in wood kilns or energy production with wood pellets. However, additive manufacturing methods for shaping beams would achieve an overall better environmental impact by eliminating waste, and could open a wider range of design options. In fact, the section could be increased to optimize for stiffness or improve the resistance of the connections where needed.

5. Next steps and conclusions

The research shows that digital fabrication can be used in combination with shape optimization to produce more efficient bending systems in timber. Once the shaping algorithm is calibrated on the material properties and the shear model refined, this method has the potential to reduce the weight of floor systems. Next, alternative fabrication methods should be developed to use the material more efficiently and open the optimization outside of the initial bounding box. Furthermore, the design space of shaped structural elements expends considerably when the shaping method could be applied to indeterminate structural systems. Shaping indeterminate structures changes their moment distribution due to the applied loads, thus creating a new design space.

Finally, the appeal for timber buildings can be increased when saving materials in ubiquitous structural elements is turned into a design opportunity. Shaping beams or structural elements becomes a new collaboration ground for designers and engineers.

References

[1] United States Energy Information Administration, https://www.eia.gov/energyexplained/?page=us_energy_home#tab3, July 2017.

[2] De Wolf, C. "Low Carbon Pathways for Structural Design: Embodied Life Cycle Impacts of Building Structures." MIT PhD Dissertation, June 2017, 218p.

[3] Spillers W. R., MacBain K. M., *Structural Optimization*, Springer, 2009.

[4] Allen E., Zalewski W., *Form and Forces – designing efficient, expressive structures*, Wiley, 2010.

[5] Engel E. *Structure Systems*, Gerd Hatje Publishers, 1997

[6] Timoshenko S. P., *History of strength of materials*, Dover Publications New York, 1983.

[7] Samyn P., *Etude de la morphologie des structures a l'aide des indicateurs de volume et de déplacement*, Academie Royale de Belgique, 2004.

[8] Aage N., Joergensen M.N., Andreasen C.S. and Sigmund O.. *Interactive topology optimization on hand-held devices*, Struct Multidisc Optim, vol. 47, No. 1, 2013, p.1-6.

[9]   Bendsoe M.P. and Sigmund O., *Topology optimization: Theory, Methods and Applications.* Springer, 2003.

[10]   Cui C., Ohmori H., Sasaki M., *Computational morphogenesis of 3D structures by extend ESO method*, International Association for Shell and Spatial Structures, vol. 44, 2003, pp. 51-61.

[11]   West M., *The fabric formwork book*, Routledge, 2016.

[12]   Guerdal Z. and Haftka R. T., *Elements of structural optimization*, Kluwer Academic Publishers, 2012.

[13]   Rhinoceros 5.0, Robert McNeel & Associates, 2015.

[14]   Grasshopper 1.0, Robert McNeel & Associates, 2014.

[15]   Floery S., Schmiedhofer H. and Reis M., *Goat – gradient-free optimization for Grasshopper®,* Version 3.0, 2010.

[16]   Hankinson, R.L. *Investigation of crushing strength of spruce at varying angles of grain*, Washington DC: US Air Service Inform, 1921 (Circular III, n 259).

[17]   Kollman, F.F.P., *Principal of Wood Science and Technology*, Volume 1, Solid Wood. Berlin: Springer-Verlag, 1984.